PHOTOEMISSION STUDY OF NANOSTRUCTURED PLASMONIC PHOTOCATHODES*

M. Bulgacheva†, E. Gjonaj, Technical University of Darmstadt, Darmstadt, Germany
D. Bazyl, Deutsches Elektronen-Synchrotron DESY, Hamburg, Germany

Abstract

We present a simulation study of a nanostructured plasmonic copper photocathode for use in the new photoinjector that is presently being developed for the high-duty-cycle operation upgrade of the European XFEL. The simulations are based on a spatially resolved photoemission model using the Fowler–DuBridge formalism and including the Schottky effect induced by the accelerating field on the cathode surface. Particle-in-cell simulations are performed to evaluate the phase-space of the beam in the near-cathode region. It is shown that while quantum efficiency is improved, photoemission from the plasmonic cathode leads to a substantially increased transverse emittance and higher energy spread of the beam compared to the case of a flat copper surface. Space-charge effects remain moderate for the operating bunch charge considered in the study.

INTRODUCTION

The future continuous-wave (CW) operation in the high-duty-cycle (HDC) mode of the European XFEL (EuXFEL) requires a robust electron source capable of delivering 100 pC electron bunches at MHz repetition rate [1, 2]. For this purpose, a new SRF L-band electron gun is currently under development at DESY in Hamburg, Germany. The new gun design is foreseen to include a novel nanostructured (NS) copper photocathode [3]. These cathodes offer enhanced quantum efficiency (QE) through improved photon absorption. This allows to reduce the required laser power and, therefore, reduce power losses and potential heating damage in the SRF gun.

Several simulation and experimental studies on NS photocathodes have been reported in recent years [4–8]. However, a self-consistent treatment of plasmonic fields, spatially resolved photoemission, and three-dimensional beam dynamics is still missing. In this paper, we present a complete emission model for NS photocathodes including all these aspects. Furthermore, we present simulation results for a copper photocathode consisting of conical nanoholes and optimized for linear photoemission at 257 nm. The basic simulation methodology was previously shortly mentioned in [3]; here we provide a detailed description of the approach and analyze the results of electromagnetic field and beam dynamics simulations for the considered photocathode.

* Work is funded by the German Ministry of Research (BMBF) under contract 005K2022
† margarita.bulgacheva@tu-darmstadt.de

METHOD

Electromagnetic Field Simulations

Plasmonic photocathodes typically consist of a periodic lattice of sub-wavelength nanoholes that are engraved on a metallic surface as shown in Fig. 1a. Such structures support surface-localized electromagnetic modes known as Surface-Plasmon-Polaritons (SPP) [9]. To increase light absorption, the shape and dimensions of the nanoholes must be optimized for SPP-resonance at the target wavelength [4]. For this purpose, we perform FDTD simulations using CST Studio Suite® [10]. The model consists of a single nanohole with periodic boundary conditions, where a linearly polarized laser is applied from above at normal incidence. We considered various types of structures consisting of conical, square and cylindrical nanoholes. As seen in Fig. 2a, conical nanoholes exhibit approximately half of the peak field strength compared to square and round geometries, while achieving equivalent absorptance. The better field uniformity makes this shape the preferable choice, as it minimizes the risk of optical damage. We therefore consider in the following only conically shaped nanostructures.

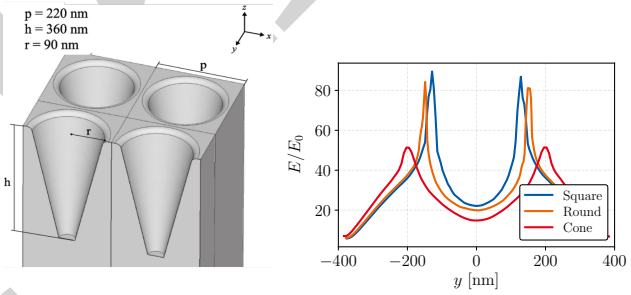

(a) (b)

Figure 1: a) Conical nanohole geometry optimized for a 257 nm laser. b) Field enhancement factor along the surface for square, round, and conical nanohole geometries.

The geometrical parameters including radius, depth and periodicity of the nanoholes are numerically optimized to minimize light reflection at the target wavelength of 257 nm. Figure 1b shows the result of this optimization for the photocathode with conical nanoholes (see also Fig. 1a for the optimal nanohole dimensions). The surface reflectance at 257 nm is reduced from 36% for a flat copper surface to less than 6% for the NS photocathode. This corresponds to an overall photon absorption rate that is ~1.5 times higher than for a flat cathode. However, as shown in Fig. 2b, the power loss density of the plasmonic mode is unevenly distributed on the cathode surface. The light absorption pattern is furthermore anisotropic as it depends on the polarization

direction of the driving laser. These observations indicate a nontrivial photoemission process that can only be quantified by a spatially resolved emission model.

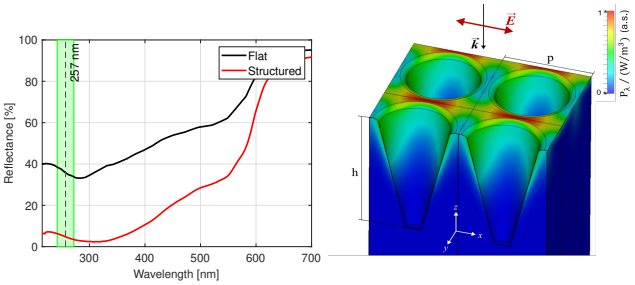

(a) (b)

Figure 2: a) Reflectance spectrum of the NS copper cathode compared to that of a flat copper surface. The nanostructure is optimized for minimum reflectance at 257 nm. b) Power loss density $P_\lambda/(W/m^3)$ in arbitrary scaling for a linearly polarized incident illumination at 257 nm.

Photoemission Model

The photocurrent density is computed from the Fowler–DuBridge model for single-photon emission [11],

$$J_r(\mathbf{r},\omega) = A\frac{e}{\hbar\omega}(1-R(\mathbf{r},\omega))I_\lambda T^2 F\left(\frac{\hbar\omega - e\Phi(\mathbf{r})}{kT}\right), \quad (1)$$

where A is the Richardson constant, e the elementary charge, T the temperature, I_λ the incident photon intensity, $R(\mathbf{r},\omega)$ the surface reflectivity, F the Fowler function, $\hbar\omega$ the photon energy, k the Boltzmann constant, and $\Phi(\mathbf{r})$ the effective work function. In the following, we assume an intrinsic work function of $\phi_w = 4.6\,\mathrm{eV}$ for copper [12], while the effective work function, $\Phi(\mathbf{r})$, depends on the local electric field strength on the surface due to the Schottky effect [13].

To compute the current density (1), we first discretize the photocathode surface using a triangular mesh. For each facet, we obtain a locally absorbed optical power by integrating the power loss density within the cathode along the inward surface normal over the optical penetration depth. The latter is defined as $\lambda_{\mathrm{opt}} = \lambda/(4\pi k)$, where k is the extinction coefficient evaluated from the Johnson & Christy complex permittivity data for copper [14]. The Schottky correction to the work function is applied locally according to

$$\Phi(\mathbf{r}) = \phi_w - e\sqrt{\frac{eE_a(\mathbf{r})}{4\pi\varepsilon_0}}, \quad (2)$$

where $E_a(\mathbf{r})$ is the accelerating field applied on the cathode surface. The electric field distribution on the surface is shown in Fig. 3a, where an applied accelerating gradient of 50 MV/m is assumed. The large field variation along the surface results in substantial work function modifications. At the top surface, the Schottky effect lowers the effective work function by approximately 7%, compared to a negligible reduction inside the nanoholes. The resulting photocurrent distribution for a single nanohole taking into account the Schottky effect is shown in Fig. 3b. The current density scales linearly with the incident laser power and is, therefore, normalized to unity. The clearly visible current concentration at the nanohole edges is consistent with the SPP-absorption pattern shown in Fig. 2b. Furthermore, for a linear laser polarization both the power loss density and the photoemission current distribution are anisotropic. However, the photoemission current distribution is not solely determined by the plasmonic field pattern on the cathode surface. It also depends on the local Schottky modification of the work function, which has a substantial impact on photoemission as will be shown below.

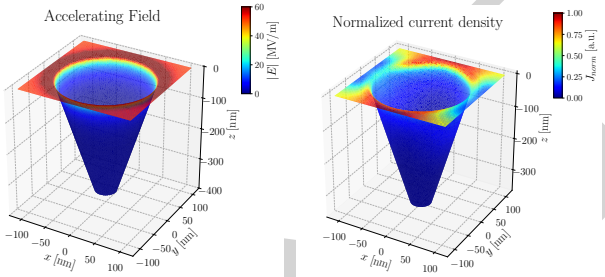

(a) (b)

Figure 3: a) Distribution of the accelerating electric field on the cathode surface for a peak applied gradient of 50 MV/m. b) Normalized photocurrent density for a linearly polarized incident illumination at 257 nm.

Emission Samples

To perform tracking simulations, we generate macroparticles on the surface mesh facets with an emission probability proportional to the local emission current (1). Using the nominal bunch parameters of the European XFEL, the incident laser intensity, $I_\lambda = I_\lambda(\mathbf{r},t)$, has a uniform radial distribution with an rms spot size of $\sigma_x = 0.25\,\mathrm{mm}$ and a Gaussian temporal profile of 18 ps rms. Rather than fixing the peak power of the laser pulse, we scale the laser intensity such that the total charge emitted from the full emission area of the photocathode is 100 pC. This reflects standard photoinjector operation, where the laser power is adjusted to the desired bunch charge. The initial kinetic energy of each emitted macroparticle is sampled uniformly in $(0, \hbar\omega - \Phi(\mathbf{r}))$. The emission angle follows a cosine distribution with respect to the local surface normal [15]. The resulting particle data are then passed at each time step to a PIC solver for tracking simulations.

SIMULATION RESULTS

Phase-space of Emitted Beam

The PIC simulations are performed for a single nanohole using periodic boundary conditions. We evaluate the particle distribution on a reference plane located a few nm above the cathode surface and then scale the resulting phase-space parameters in postprocessing to the full laser spot size. Figure 4 shows the normalized transverse emittance and rms

energy spread as a function of photon energy for the flat and NS photocathodes, respectively. The NS cathode exhibits a clear asymmetry between the x- and y-directions, where the former is aligned with the laser polarization (cf. also Fig. 5). At the target wavelength of 257 nm, the NS cathode features an emittance increase by a factor of approximately 2 relative to the flat surface when the Schottky correction is included. This is attributed to the inhomogeneous emission current distribution induced by SPP-field localization at the nanohole edges as seen in Fig. 2b.

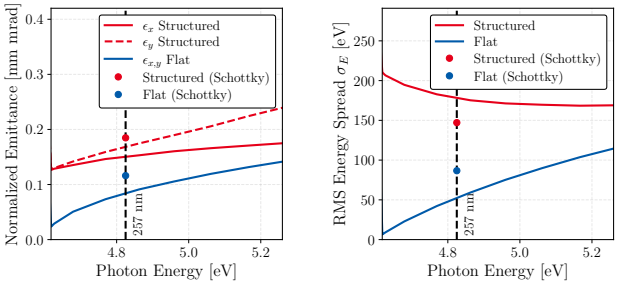

Figure 4: Transverse normalized emittance (left) and energy spread (right) of the emitted beam vs. photon energy for flat and NS copper photocathodes.

The energy spread of the beam is substantially larger for the NS cathode compared to the flat one. This effect is particularly pronounced at lower photon energies approaching the single-photon emission threshold. This behavior is attributed to the reduced energy of electrons emitted from the nanohole depth. These electrons experience weak acceleration and, therefore, form a low-energy tail in the longitudinal phase space as shown in Fig. 5.

The Schottky effect affects the NS and flat cathode cases differently. For the flat cathode, the reduced work function increases particle energy and therefore the energy spread. In the NS photocathode case, the Schottky effect enhances emission from the planar top surface only, where the accelerating field is strongest. As a result, the relative contribution of the low-energy tail coming from the nanohole interior is reduced. This leads to a slight decrease in energy spread compared to the case when the Schottky effect is neglected. A detailed view of the phase-space of the emitted beam for laser illumination at 257 nm is shown in Fig. 5.

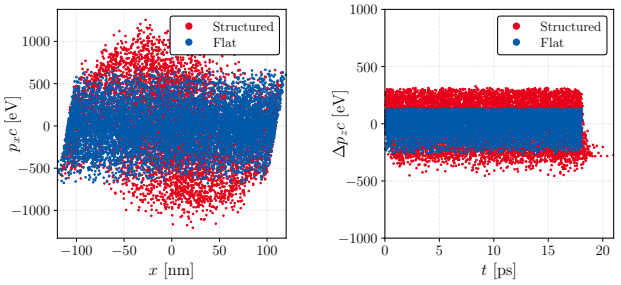

Figure 5: Horizontal (left) and longitudinal (right) phase space of the emitted beam at 257 nm.

Effect of Space-Charge

The effect of space-charge fields for the considered initial bunch charge of $Q_b = 100$ pC is expected to be quite weak. As shown in Fig. 6, including space-charge in the simulations leads to a small reduction of the emitted charge by approximately 2%. This appears to happen mainly because of the loss of low-energy particles emitted from inside the nanoholes. This charge loss remains small because the emission probability inside the nano-cone is substantially lower than at the top surface. The resulting emitted charge profile from the NS photocathode, when space-charge is taken into account, is shown in Fig. 6.

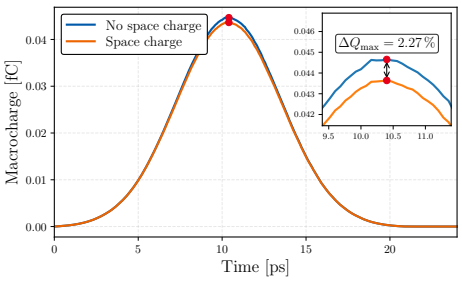

Figure 6: Emitted charge profile from the NS photocathode with and without space-charge effect.

CONCLUSION

We have presented a simulation study of a nanostructured plasmonic copper photocathode. The cathode consists of a periodic lattice of conical nanoholes optimized for UV illumination at 257 nm. Electromagnetic simulations demonstrate a sixfold reduction of surface reflectance relative to a flat copper cathode. This corresponds to a 1.5-fold increase of QE when the Schottky effect is not accounted for. We have furthermore developed a spatially resolved Fowler–DuBridge emission model, including the local Schottky correction to the work function. Beam dynamics simulations using this model show that nanostructuring results in a substantially increased normalized emittance and rms energy spread of the emitted beam. For the considered NS photocathode, the transverse emittance of the beam is ~2 times higher than in the case of a flat copper surface. Furthermore, for a linear laser polarization, the transverse phase-space is asymmetric, while the longitudinal phase space exhibits a characteristic low-energy tail corresponding to particles emitted at the nanohole depth. Space-charge effects are negligible for the European XFEL bunch of 100 pC. Overall, these results indicate that NS photocathodes operated in the linear emission regime offer enhanced quantum efficiency at the cost of phase-space deterioration. This must be taken into account in further SRF-gun and photoinjector design studies.

REFERENCES

[1] W. Decking *et al.*, "A MHz-repetition-rate hard X-ray free-electron laser driven by a superconducting linear accelerator",

Nat. Photonics, vol. 14, pp. 391–397, 2020. doi:10.1038/s41566-020-0607-z

[2] D. Bazyl, Y. Chen, M. Dohlus, and T. Limberg, "CW Operation of the European XFEL: SC-Gun Injector Optimization, S2E Calculations and SASE Performance", Nov. 2021. doi:10.48550/arXiv.2111.01756

[3] D. Bazyl *et al.*, "Overview of metal cathode R&D for the CW L-band SRF photoinjector at DESY", in *Proc. SRF'25*, Tokyo, Japan, Sep 2025, paper TUP65. doi:10.18429/JACoW-SRF2025-TUP65

[4] P. Musumeci *et al.*, "Multiphoton Photoemission from a Copper Cathode Illuminated by Ultrashort Laser Pulses in an RF Photoinjector", *Phys. Rev. Lett.*, vol. 104, p. 084801, 2010. doi:10.1103/PhysRevLett.104.084801

[5] R. K. Li *et al.*, "Surface-plasmon resonance-enhanced multiphoton emission of high-brightness electron beams from a nanostructured copper cathode", *Phys. Rev. Lett.*, vol. 110, 2013. doi:10.1103/PhysRevLett.110.074801

[6] Z. Jiang *et al.*, "Monte Carlo simulations of electron photoemission from plasmon-enhanced bialkali photocathode", *Phys. Rev. Accel. Beams*, vol. 24, 3, p. 033402, 2021. doi:10.1103/PhysRevAccelBeams.24.033402

[7] C. M. Pierce *et al.*, "Experimental characterization of photoemission from plasmonic nanogroove arrays", *Phys. Rev. Appl.*, vol. 19, p. 034034, 2023. doi:10.1103/PhysRevApplied.19.034034

[8] Z. Zhang *et al.*, "Surface-plasmon enhanced photoemission of a silver nano-patterned photocathode", *Nucl. Instr. Meth. Phys. Res. Sec. A*, vol. 865, pp. 114-118, 2017. doi:10.1016/j.nima.2016.11.042

[9] W. Barnes, A. Dereux, and T. Ebbesen, "Surface plasmon subwavelength optics", *Nature*, vol. 424, pp. 824–830, 2003. doi:10.1038/nature01937

[10] CST Studio Suite, http://www.cst.com/.

[11] K. L. Jensen, *Introduction to the Physics of Electron Emission*, John Wiley & Sons, 2017.

[12] H. B. Michaelson, "The work function of the elements and its periodicity", *J. Appl. Phys.*, vol. 48, no. 11, pp. 4729–4733, 1977. doi:10.1063/1.323539

[13] D. H. Dowell and J. F. Schmerge, "Quantum efficiency and thermal emittance of metal photocathodes", *Phys. Rev. Spec. Top. Accel. Beams*, vol. 12, p. 074201, 2009. doi:10.1103/PhysRevSTAB.12.074201

[14] P. B. Johnson and R. W. Christy, "Optical constants of the noble metals", *Phys. Rev. B*, vol. 6, pp. 4370-4379, 1972. doi:10.1103/PhysRevB.6.4370

[15] W. J. Smith, *Modern Optical Engineering: The Design of Optical Systems*, McGraw-Hill, 2000.